

Optimizing Polyphase-Coded FM Waveforms within a LINC Transmit Architecture

Lane Ryan^{1,2}, John Jakabosky¹, Shannon D. Blunt¹, Christopher Allen¹, and Lawrence Cohen³

¹ Radar Systems Lab, University of Kansas, Lawrence, KS

² Honeywell FM&T, Kansas City, MO

³ Radar Division, US Naval Research Laboratory, Washington, DC

Abstract—Linear amplification using nonlinear components (LINC) is a design approach used to mitigate the nonlinear distortion introduced by the transmitter components, particularly the high-power amplifier. This work investigates using the LINC approach in combination with a new polyphase-coded FM (PCFM) waveform optimization strategy to strike a balance between waveform effectiveness, power efficiency, and spectral containment. A hardware-in-the-loop optimization of LINC-PCFM waveforms is employed to enable joint consideration of the transmitter components and the excitation waveforms.

I. INTRODUCTION

For a radar system, the transmitter dominates the system's overall power consumption, determines its maximum operating range, and establishes the spectral content of the radiated emissions. These factors make decisions regarding the transmitter components/topology and the excitation waveform vital to the desired performance of the overall system. In particular, radar usage of the RF spectrum [1,2] continues to be highly contested by other prospective spectrum users (e.g. commercial communications) and there is every indication that this pressure will only increase. As such, there is an ongoing debate about how to best modify the existing Radar Spectrum Engineering Criteria (RSEC) to enforce a much higher degree of spectral containment through sharper spectral roll-off (20 dB/decade may increase to 30 or even 40 dB/decade) and with a lower out-of-band limit of at least 60 dB relative to the peak power at the carrier frequency. This prospect creates some unique challenges for the design of radar transmitters and their emissions [3].

There has been considerable research in the area of waveform design and optimization (e.g. [4-7] and references therein). While frequency-modulated (FM) waveforms are attractive from a physical implementation standpoint (e.g. via surface acoustic wave (SAW) device or arbitrary waveform generator (AWG)), the inherent structure of codes is attractive because optimization can be readily performed by searching over the parameters of the code space. Furthermore, the recent development of a scheme for the physical implementation of arbitrary polyphase codes as continuous waveforms now makes it feasible to optimize FM waveforms directly. Based on the continuous phase modulation (CPM) framework used in some digital communication standards that require strict power and spectral efficiency, these new

polyphase-coded FM (PCFM) radar waveforms are not only amenable for use with a high-power transmitter, they can even be optimized with the hardware-in-the-loop to be specially tuned to the idiosyncrasies (i.e. distortion) of a specific transmitter [8-10]. As such, the impact of different transmitter components and topologies can now be considered jointly with the waveform in a holistic manner. Here we take such an approach for a particular instantiation of the general LINC paradigm that employs a 180° coupler [11,12].

To maximize power efficiency and thus energy-on-target, a common radar requirement is for the transmitter power amplifier (PA) to be operated in saturation. The constant modulus and relatively bandlimited attributes of FM waveforms (such as PCFM) naturally helps to negate most of the effects of operating in the nonlinear regime of the PA. However, this nonlinearity also precludes the use of an amplitude taper to increase the spectral containment of the transmitted waveform by “slowing down” the otherwise rapid rise/fall-time of the pulse. The LINC strategy addresses this issue by using two matched power amplifiers. The amplifier outputs are combined in a 180° coupler, with their relative phases determining the amplitude of the resulting waveform.

The LINC approach is a powerful tool that allows for the creation of waveforms that could not be easily implemented with a single amplifier design. With this setup, it is possible to apply an amplitude taper to a pulse without experiencing the negative nonlinear effects of the components involved. Tapering is well known as a means to reduce range sidelobes for a linear FM (LFM) chirp [4]. The difficulty is that tapers are very problematic to implement with a single saturated amplifier. However, if the output amplitudes of two parallel amplifiers can be calibrated to match reasonably well, then amplitude manipulation of the resulting emission can be attained through phasing in/out of the two input waveforms.

The issue being addressed is application driven and very specific to the design requirements of a given radar system. If spectral containment is not a high priority, then this approach is of less value. However, if the spectral allocation is very tight, then the dual amplifier approach becomes quite valuable. Without increasing the complexity of the system, an obvious alternative solution would be to simply back off the power and operate a single transmitter amplifier in a linear region of its output curve. This alternative is typically not an acceptable solution due to the degradation in output power and

power efficiency. What makes the LINC technique so useful is that it effectively mimics a linear amplifier while retaining the high power efficiency and thus most of the high output power (relative to the original sharp rise/fall-time some power is still lost due to amplitude tapering the pulse edges).

II. LINC-PCFM RADAR IMPLEMENTATION

Continuous phase modulation (CPM) is used in a variety of applications such as aeronautical telemetry and deep-space communications and forms the basis of the Bluetooth wireless standard. The primary advantages of CPM are good power efficiency (constant modulus) and good spectral efficiency (tight spectral roll-off). Both of these factors are very important to radar systems in order to get the most energy on target while maintaining required spectral containment. The CPM framework, modified to implement polyphase radar codes and thereby generate polyphase-coded FM (PCFM) waveforms [8,9], is shown in Fig. 1.

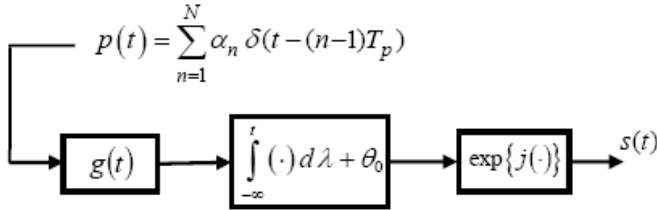


Figure 1. PCFM radar waveform implementation

The input $p(t)$ is a train of N impulses with separation T_p such that the total pulsewidth is $T=NT_p$. The phase change between successive chips in the code is defined as

$$\alpha_n = \begin{cases} \tilde{\alpha}_n & \text{if } |\tilde{\alpha}_n| \leq \pi \\ \tilde{\alpha}_n - 2 \text{sgn}(\tilde{\alpha}_n) & \text{if } |\tilde{\alpha}_n| > \pi \end{cases} \quad (1)$$

where

$$\tilde{\alpha}_n = \theta_n - \theta_{n-1} \quad \text{for } n=1, \dots, N, \quad (2)$$

and θ_n is the phase of the n^{th} element in a length of $N+1$ polyphase code. The resulting baseband output $s(t)$ is a form of nonlinear FM (NLFM) that can be modulated onto a carrier.

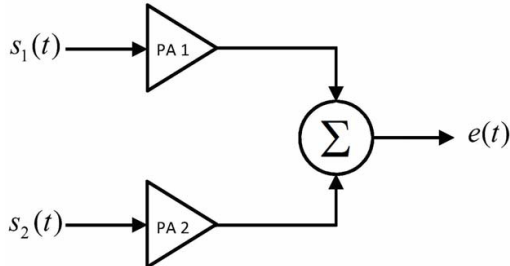


Figure 2. 180° coupler LINC transmitter implementation

For the LINC configuration considered here, two continuous waveforms $s_1(t)$ and $s_2(t)$ are generated such that their relative phases, when combined in a 180° coupler (see Fig. 2), creates a phase-modulated pulse $e(t)$ whose amplitude follows some desired shape (e.g. a Tukey window) for the purpose of controlling the spectral content induced by the

pulse rise/fall-time. By controlling the relative phase of $s_1(t)$ and $s_2(t)$, as shown in Fig. 3, the amplitude tapering of $e(t)$ is produced (see Fig. 6). To generate the tapering effect, waveform $s_2(t)$ is modified with respect to waveform $s_1(t)$ at the beginning and end of the pulse by changing the associated values of α_n for the 2nd waveform.

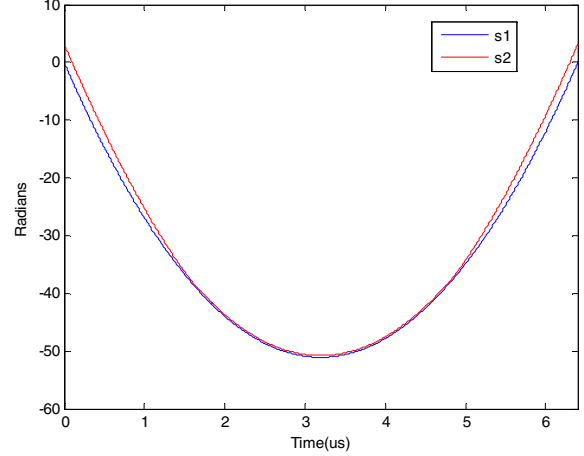


Figure 3. Unwrapped phase of waveforms $s_1(t)$ and $s_2(t)$

The hardware configuration for the transmitter-in-the-loop optimization is shown in Figure 4.

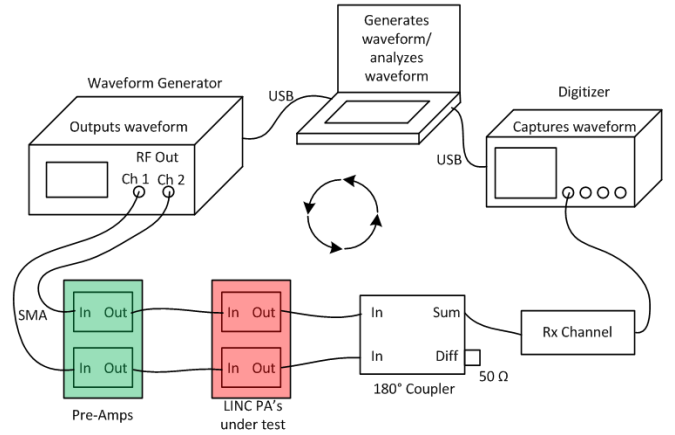


Figure 4. Hardware configuration

Mathematically, this implementation can be represented as follows:

$$s_1(t) = s(t) \quad (3)$$

$$s_2(t) = s(t) \exp\{j\phi(t)\} \quad (4)$$

where

$$\phi(t) = \cos^{-1}(2w^2(t)-1) \quad (5)$$

is the phase adjustment for $s_2(t)$ and $w(t)$ is the window. The output waveform $e(t)$ is thus

$$e(t) = s_1(t) + s_2(t) = s(t)w(t) \exp\{j\psi(t)\}, \quad (6)$$

where

$$\psi(t) = \tan^{-1} \frac{\sqrt{1-w^2(t)}}{w^2(t)} \quad (7)$$

is a residual phase response that is produced as a by-product when combining the two waveforms of (3) and (4) within this LINC configuration. Because the amplitude weighting and associated phase response modify the underlying waveform $s(t)$ in (6), it is necessary to optimize the output emission $e(t)$ according to the desired specifications (e.g. peak sidelobe level, integrated sidelobe level, range resolution, etc.).

III. EMISSION OPTIMIZATION

While the integration of a pulse tapering effect to control pulse rise/fall-time is beneficial from a spectral containment perspective, it also introduces changes to the waveform that can be expected to degrade optimized range sidelobes. The solution is to optimize with the LINC topology “in the loop”.

To perform optimization, the waveform $e(t)$ from Fig. 2 is injected via loopback into the receiver and captured by a digitizer. The optimization is driven by minimizing the peak sidelobe level (PSL) of the emission autocorrelation and is facilitated by searching over the parameter space defined by the set of α_n values. This approach [8,10] ties together the optimization of the discrete code with the often ignored physical effects of the transmitter (here including the LINC-enabled tapering) as illustrated in Fig. 5.

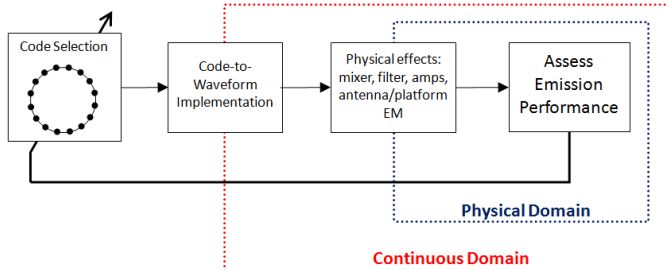


Figure 5. Transmitter-in-the-loop emission optimization

The optimization scheme used here employs a greedy search strategy [8,10] that does not guarantee the global minimum but has been shown to yield quite good solutions nonetheless. The global minimum cannot be guaranteed because the PSL cost function is not convex and an exhaustive search is not feasible as the number of unique waveforms is exceedingly high. For example, for $N = 64$ phase transitions in the code and $M = 64$ possible phase states there are $M^N = 64^{64} = 3.9402 \times 10^{115}$ possible unique waveforms.

For the optimization, first a “phase change” version of the code, defined as $\mathbf{x} = [\alpha_1 \alpha_2 \dots \alpha_N]$, is initialized with some starting phase sequence. Using the CPM implementation from Fig. 1, a PCFM waveform is then generated from this code. Third, α_1 is cycled through every possible phase change within a discrete sampling over $[-\pi, \pi]$, with the value generating the lowest PSL being kept. The 2nd and 3rd steps are then repeated with $n = 2, 3, \dots, N$ until no single value of α_n can be changed

to provide a lower PSL. This greedy approach has a search space on the manageable order of MN as opposed to M^N .

Since it is not an exhaustive search, the effectiveness of the hardware-in-the-loop optimization does depend on the initial code that is used to seed the search algorithm. As such, the optimization is performed in two stages. The first stage involves optimization with the hardware effects emulated in simulation. Here this simulation is seeded with an LFM chirp (P3 code converted into phase change format). The starting code is not nearly as important in simulation because very fast optimization can be performed in the simulation environment (e.g. at present roughly 17,000 waveforms can be analyzed per second using a high-performance GPU). By comparison, for the test equipment employed in this experiment, only one waveform can be analyzed every 1.5 seconds when the actual transmitter hardware is included. The bottleneck is mostly due to the speed at which the waveform generator can upload each new candidate waveform. This time constraint enforced by the hardware suggests that the hardware-in-the-loop optimization should be seeded with a waveform previously optimized in simulation so as to start out in the general neighborhood of a good result.

IV. SIMULATION & EXPERIMENTAL RESULTS

Here a Tukey window is used to taper the rise/fall-time of a 64 μs pulse. To achieve the desired degree of spectral containment, the transition length of the taper is 16 chips each at the beginning and end of the pulse, which is comprised of a total of $N = 64$ chip transitions. This amplitude taper produces a 3.2 dB loss in SNR, though the transition length could be shortened depending on spectral containment requirements. For example, a window using a transition length of 4 chips will only decrease SNR by 0.7 dB.

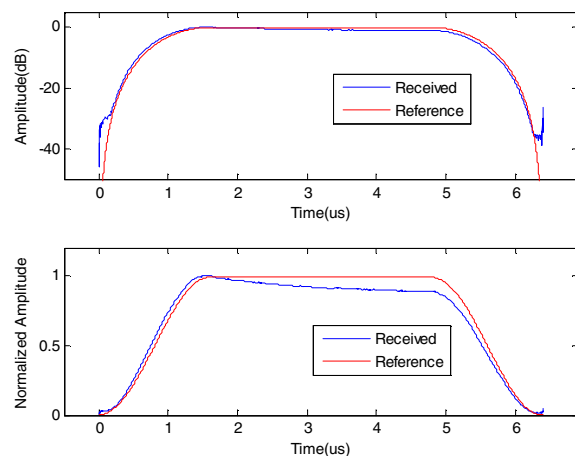


Figure 6. Received pulse amplitude

Figure 6 depicts the hardware-generated (received) and simulated reference pulse amplitudes. In the log scale plot of Fig. 6, it is shown that the only significant deviations from the reference trace are below -30 dB. In the linear scale plot of Fig. 6, it is easier to see a gradual downward slope present in what should be the flat portion of the pulse, which is likely due to the amplifiers not having an entirely linear gain

throughout the frequency band being used. It is important to note that the PAs are being operated roughly 7 dB beyond their 1 dB compression point.

While the taper generated by the LINC implementation can “slow down” the rise/fall-time as shown in Fig. 6, the subsequent emission $e(t)$ requires optimization to provide sufficiently low range sidelobes. Figure 7 shows the autocorrelation of a simulated PSL-based optimization of the tapered emission compared to a Tukey-tapered LFM (the initialization). The Tukey tapered LFM waveform has a PSL of -16.38 dB, while the optimized, tapered waveform yields a PSL of -41.44 dB, a 25 dB improvement.

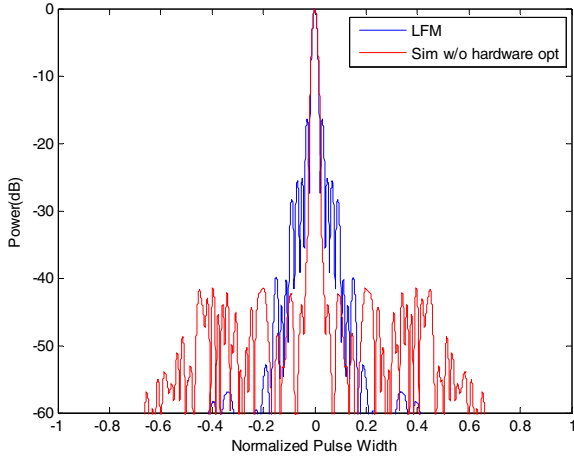


Figure 7. LFM and optimized PCFM

Next, hardware-in-the-loop optimization was performed using the simulation-optimized waveform as an initialization. Shown in Figure 8 are a hardware-in-the-loop optimized PSL of -42.81 dB compared to the simulation-optimized PSL of -41.45 dB, a modest improvement of 1.36 dB.

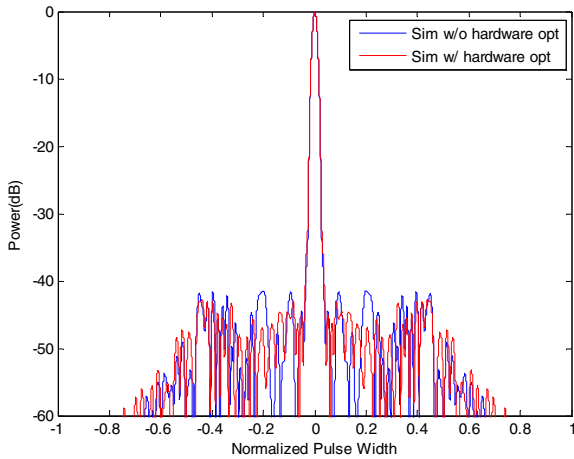


Figure 8. Simulation-optimized and hardware-in-the-loop optimized PCFM

Figures 9-11 illustrate the spectrum of the LFM waveform, the simulation-optimized waveform, and the hardware-in-the-loop optimized waveform, each with and without the tapering effect. All of the waveforms are captured on a spectrum analyzer after being driven through the transmitter (in either

normal or 180° coupler configuration). In each figure, the higher trace represents the transmitted waveform without the Tukey taper applied.

The vertical scale for all three figures is 10dB/division with a frequency span of 110 MHz. It is easy to see that the out-of-band spectral content is being suppressed by 15-20 dB until reaching the noise floor of this particular spectrum analyzer. Examining Figs. 10 and 11, is interesting to note that the optimization process also recovers some of the lost bandwidth of the tapered LFM waveform (Fig. 8).

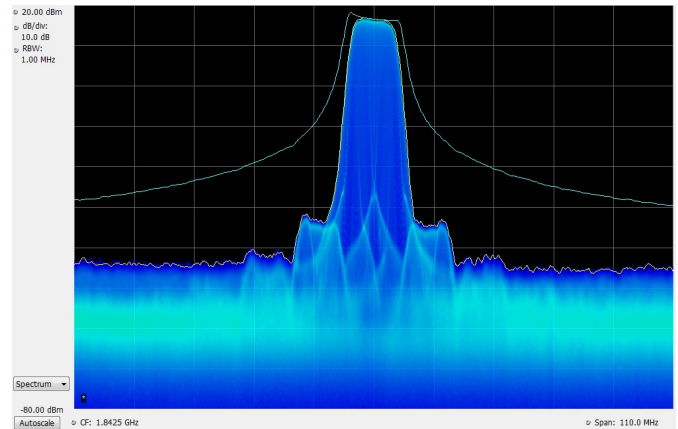


Figure 9. LFM spectrum with and without Tukey 16 taper

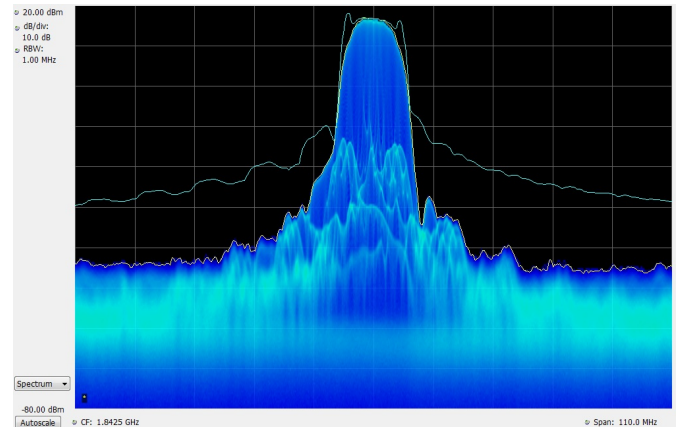


Figure 10. Simulation-optimized spectrum with and without Tukey 16 taper

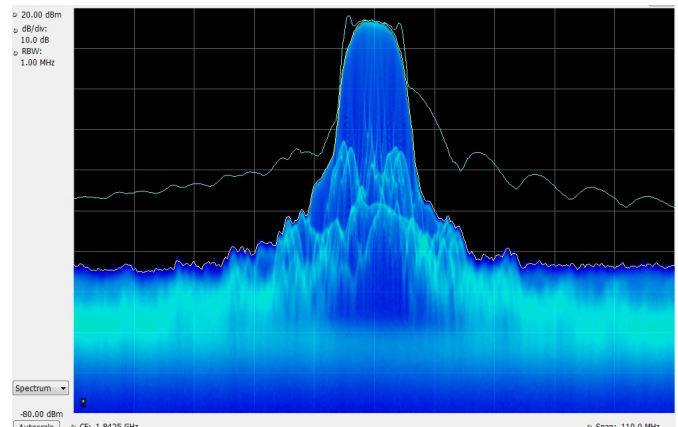


Figure 11. Hardware-optimized spectrum with and without Tukey 16 taper

The previous example utilized a 16 chip taper length at the beginning and end of the pulse such that half the pulse has some degree of taper applied. However, significant spectral containment can still be achieved even with a much shorter taper. For the sake of comparison, Figs. 12-14 show the transmitted spectrum with and without a 4 chip taper for LFM, simulation optimized, and hardware optimized.

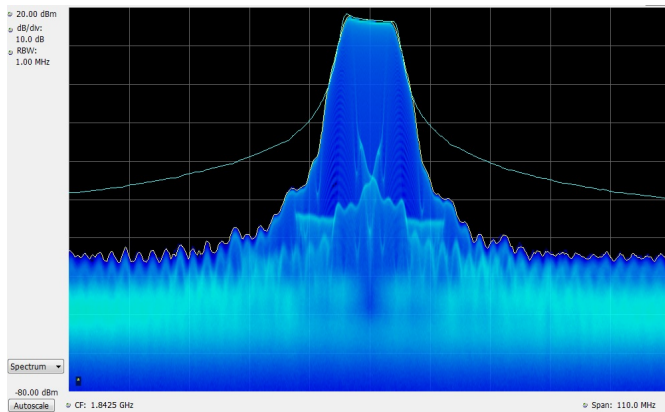


Figure 12. LFM spectrum with and without Tukey 4 taper

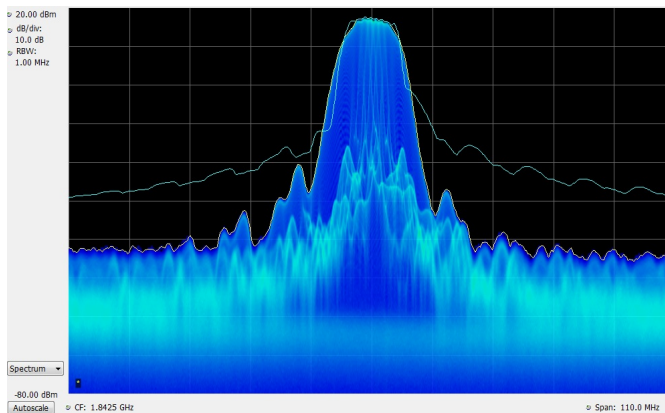


Figure 13. Simulation-optimized spectrum with and without Tukey 4 taper

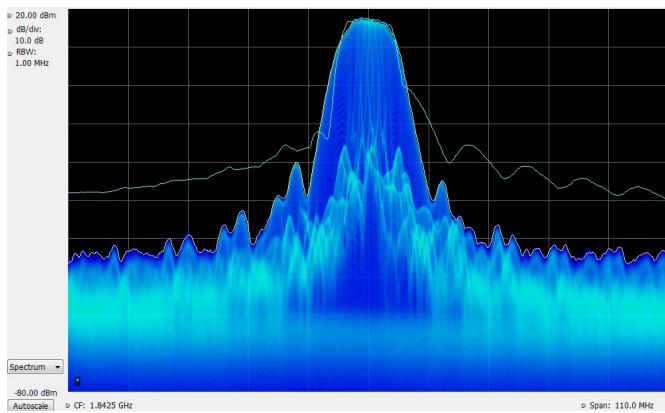


Figure 14. Hardware-optimized spectrum with and without Tukey 4 taper

CONCLUSIONS

A robust waveform optimization scheme using the LINC approach was successfully developed as supported by experimental results. This process is resilient to transmitter PA distortion and provides a means with which to achieve spectral containment with high power efficiency. The implementation of the Tukey window allows the pulse rise/fall-time to be easily adjustable. Ongoing work is examining various other LINC topologies within this general transmitter/waveform co-design framework. Furthermore, recent results on waveform “over-coding” [13] may provide greater degrees-of-freedom with which to contend with non-ideal/nonlinear transmitter effects.

REFERENCES

- [1] *Manual of Regulations and Procedures for Federal Radio Frequency Management*, NTIA, May 2011 Revision of January 2008 Edition.
- [2] *ITU Manual of Radio Regulations*, No.119-08-Rev.1, 6 October 2008.
- [3] H. Griffiths, S. Blunt, L. Cohen, and L. Savy, “Challenge problems in spectrum engineering and waveform diversity,” *IEEE Radar Conference*, Ottawa, Canada, 29 Apr. – 3 May 2013.
- [4] N. Levanon, E. Mozeson, *Radar Signals*, Wiley – IEEE Press, 2004.
- [5] M. Wicks, E. Mokole, S. Blunt, R. Schneible, and V. Amuso, *Principles of Waveform Diversity & Design*, SciTech Publishing, 2010.
- [6] S. Pillai, K.Y. Li, I. Selesnick, and B. Himed, *Waveform Diversity: Theory & Applications*, McGraw-Hill, 2011.
- [7] F. Gini, A. De Maio, and L.K. Patton, *Waveform Design and Diversity for Advanced Radar Systems*, IET, 2012.
- [8] J. Jakabosky, S.D. Blunt, M.R. Cook, J. Stiles, and S.A. Seguin, “Transmitter-in-the-loop optimization of physical radar emissions,” *IEEE Radar Conference*, Atlanta, GA, 7-11 May 2012.
- [9] S.D. Blunt, M. Cook, J. Jakabosky, J. de Graaf, and E. Perrins, “Polyphase-coded FM (PCFM) radar waveforms, part I: implementation,” to appear in *IEEE Trans. Aerospace & Electronic Systems*.
- [10] S.D. Blunt, J. Jakabosky, M. Cook, J. Stiles, S. Seguin, and E.L. Mokole, “Polyphase-coded FM (PCFM) radar waveforms, part II: optimization,” to appear in *IEEE Trans. Aerospace & Electronic Systems*.
- [11] F.H. Raab, P. Asbeck, S. Cripps, P.B. Kenington, Z.B. Popovic, N. Potheary, J.F. Sevic, and N.O. Sokal, “Power amplifiers and transmitters for RF and microwave,” *IEEE Trans. Microwave Theory & Techniques*, vol. 50, no. 3, pp. 814-826, Mar. 2002.
- [12] C. Baylis, M. Moldovan, L. Wang, and J. Martin, “LINC power amplifiers for reducing out-of-band spectral re-growth: a comparative study,” *IEEE Wireless and Microwave Technology Conference*, Melbourne, FL, 12-13 Apr. 2010.
- [13] J. Jakabosky, S.D. Blunt, and B. Himed, “Optimization of “over-coded” radar waveforms,” *IEEE Radar Conf.*, Cincinnati, OH, 19-23 May 2014.